

## **A MAXWELL GARNETT MODEL FOR DIELECTRIC MIXTURES CONTAINING CONDUCTING PARTICLES AT OPTICAL FREQUENCIES**

**M. Y. Koledintseva, R. E. DuBroff, and R. W. Schwartz**

University of Missouri-Rolla  
1870 Miner Circle, Rolla, Missouri 65409-0040, U.S.A.

**Abstract**—Mathematical modeling of composites made of a dielectric base and randomly oriented metal inclusions is considered. Different sources of frequency-dependent metal conductivity at optical frequencies are taken into account. These include the skin-effect, dimensional (length-size) resonance of metal particles, and the Drude model. Also, the mean free path of electrons in metals can be smaller than the characteristic sizes of nanoparticles, and this leads to the decrease in conductivity of the metal inclusions. These effects are incorporated in the Maxwell Garnett mixing formulation, and give degrees of freedom for forming desirable optical frequency characteristics of composite media containing conducting particles.

### **1. INTRODUCTION**

Engineering composite materials with desirable electromagnetic properties for different applications from radio frequencies to the optical range has become one of the most important problems of modern science and technology.

There are many different effective medium theories used for modeling electromagnetic properties of composites. One of them is the Maxwell Garnett model [1], which is simple and convenient for modeling due to its linearity. The Maxwell Garnett model is valid for dielectric composites with dilute conductive phases (below the percolation threshold). This is a model that implies the quasistatic approximation. Its main features are

- the mixture is electrodynamically isotropic;
- the mixture is linear, that is, none of its constitutive parameters depends on the intensity of electromagnetic field;

- the mixture is non-parametric, that is, its parameters do not change in time according to some law as a result of external forces — electrical, mechanical, etc.;
- inclusions are separated by distances greater than their characteristic size;
- the characteristic size of inclusions is small compared to the wavelength in the effective medium;
- inclusions are arbitrary randomly oriented ellipsoids;
- if there are conducting inclusions, their concentration should be lower than the percolation threshold.

The Maxwell Garnett mixing rule has been successfully applied to engineering microwave absorbing materials containing carbon particles [2], using the formula for the effective relative permittivity,

$$\varepsilon_{ef} = \varepsilon_b + \frac{\frac{1}{3} \sum_{i=1}^n f_i (\varepsilon_i - \varepsilon_b) \sum_{k=1}^3 \frac{\varepsilon_b}{\varepsilon_b + N_{ik}(\varepsilon_i - \varepsilon_b)}}{1 - \frac{1}{3} \sum_{i=1}^n f_i (\varepsilon_i - \varepsilon_b) \sum_{k=1}^3 \frac{N_{ik}}{\varepsilon_b + N_{ik}(\varepsilon_i - \varepsilon_b)}}, \quad (1)$$

where  $\varepsilon_b$  is the relative permittivity of a base dielectric;  $\varepsilon_i$  is the relative permittivity of the  $i$ -th type of inclusions;  $f_i$  is the volume fraction occupied by the inclusions of the  $i$ -th type;  $N_{ik}$  are the depolarization factors of the  $i$ -th type of inclusions, and the index  $k = 1, 2, 3$  corresponds to  $x, y$ , and  $z$  Cartesian coordinates. Equation (1) is generalized for a multiphase mixture schematically shown in Figure 1. The constitutive parameters of the base material and inclusions can be functions of frequency.

Formulas for calculating depolarization factors of ellipsoids and the table of depolarization factors for canonical spheroids (spheres, disks, and cylinders) can be found in [3]. Equation (1) allows that within the same composite material, particles can have different depolarization factors. However, in reality it is almost impossible to have perfect ellipsoidal or spheroidal particles, so, for any arbitrary shape a reasonable approximation is needed. If the inclusions are thin rods (cylinders), two of their depolarization factors are close to  $N_{i1,2} \approx 1/2$ , and the third depolarization factor can be calculated as in [4],  $N_{i3} \approx (1/a)^2 \ln(a)$ . Herein,  $a = l/d$  is the aspect ratio of an inclusion of length  $l$  and diameter  $d$ . The sum of all three depolarization factors is always unity.

The dielectric properties of the conducting inclusions are described

by the complex relative permittivity

$$\varepsilon_i(j\omega) = \varepsilon'_i - j\varepsilon''_i = \varepsilon'_i - j\frac{\sigma_i}{\omega\varepsilon_0}, \quad (2)$$

the real part of which is much smaller than the imaginary part ( $\varepsilon'_i \ll \sigma_i/(\omega\varepsilon_0)$ ). In (2),  $\sigma_i$  is the bulk conductivity of inclusions.

It has been shown that by varying conductivity, aspect ratio, and concentration of inclusions it is possible to form the desirable frequency characteristics, including shielding effectiveness of composites at microwave frequencies [2]. Application of the genetic algorithms allows for optimization of the mixture contents to achieve the highest possible shielding effectiveness [5].

Mixtures of randomly oriented nanosize conducting particles at concentrations far below the percolation threshold can still be treated using Maxwell Garnett formalism at optical frequencies, but some corrections in the model must be introduced. Thus, the model should take into account peculiarities of the conductive particles' behavior at optical frequencies, which may differ considerably from their behavior at microwave frequencies. Also, dimensional resonance in the inclusion particles might greatly influence the effective permittivity of the composite.

The structure of the paper is the following. Section 2 contains the mathematical model of the composite taking the abovementioned effects into account. The results of calculations based on this model are presented and discussed in Section 3. The conclusions are summarized in Section 4.

## 2. MATHEMATICAL MODEL

### 2.1. Renormalized Conductivity Taking the Skin Effect into Account

At microwave frequencies, the skin effect in conducting inclusions can be neglected. However, at optical frequencies currents induced by the electromagnetic waves in the conducting particles exist only in very thin surface layers, while the bulk of the particle is not involved in interaction. For this reason, the skin effect is substantial and influences the frequency dependence of the particle.

Skin depth is calculated as

$$\delta(\omega) = \sqrt{\frac{2}{\omega\mu_i\mu_0\sigma_i}}. \quad (3)$$

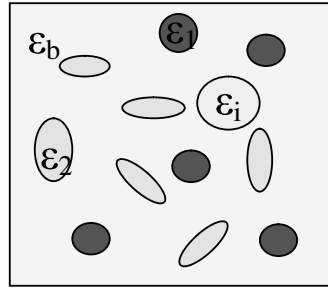


**Figure 1.** Schematic of a multiphase mixture.

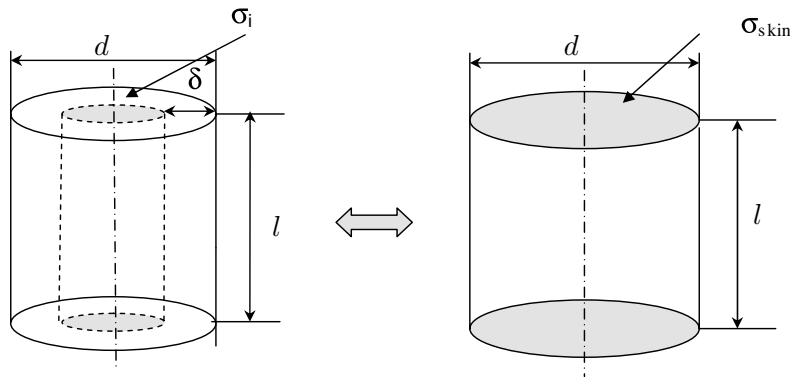


**Figure 2.** Renormalization of conductivity due to the skin-effect.

Lagarkov and Sarychev [6], according to [7, Section 61], introduced the renormalized conductivity to take the skin effect into account (see Figure 2). Renormalized conductivity is related to the bulk conductivity as

$$\begin{aligned}
 \sigma_{skin} &= \sigma_i \cdot f(\Delta); \\
 \Delta &= d / (2\delta(\omega)); \\
 f(\Delta) &= \frac{1-j}{\Delta} \cdot \frac{J_1((1+j)\Delta)}{J_0((1+j)\Delta)},
 \end{aligned} \tag{4}$$

where  $J_{0,1}$  are the Bessel functions of the zero and the first order, respectively. This renormalized conductivity appears to be a complex value, and it is dependent on frequency through  $\delta(\omega)$ . This is the basic difference between the microwave and optical behavior of metals: the conductivity of metals at optical frequencies is not constant, it depends

on frequency.

$$\sigma_{skin}(\omega) = \sigma'_{skin}(\omega) + j\sigma''_{skin}(\omega). \quad (5)$$

The real part of conductivity is responsible for  $\varepsilon''$ , while the imaginary part contributes to  $\varepsilon'$ .

## 2.2. Conductivity Taking into Account Small Size of Nanorods Compared to Mean Free Path of Electrons

Since the inclusions of interest are nanorods, they are so thin that their diameter could be smaller than the electron mean free path. Then, instead of the bulk conductivity, the corrected conductivity should be taken into account,

$$\sigma_{free} = \Lambda\sigma_i. \quad (6)$$

where the coefficient  $\Lambda$  is a function of the ratio

$$\Lambda = f(b_i/L_{free}), \quad (7)$$

where  $b_i$  is the inclusion characteristic size ( $d \leq b_i \leq l$ ) along the vector of the electric field acting on the mixture, and  $L_{free} = v_F\tau_0$  is the mean free path for electrons in the conductor [8].

For randomly oriented conducting particles, it can be assumed that the one-third of all particles have their characteristic dimension in the direction of the incident electric field close to  $b_i \approx d$ , which leads to the decrease of conductivity up to two times. One-third of all particles have  $b_i > L_{free}$ , so that their conductivity is close to the bulk conductivity. And the remainder have an average characteristic dimension of  $b_i = \frac{l+d}{2}$ , which can lead to some decrease of conductivity. Thus, the coefficient  $\Lambda$  may be even smaller than is given in the tables in [8], if the surface roughness and grain size of metal inclusion are taken into account [9–11]. For our computations, we assume that a reasonable value is  $\Lambda = 0.8$ , corresponding to a 20% decrease in conductivity. In [11, Fig. 1], it is shown that when the technology node in modern nanometer scale IC design decreases in size and becomes comparable to the mean free path of electrons in metals (for the majority of metals, such as Cu, Ag, Pt, Au, Al, etc., it is in the range of 10–100 nm at room temperature), the resistivity of metal components substantially increases, since surface, grain boundary, and barrier layer effects become noticeable.

In such cases, it is reasonable to replace the bulk conductivity  $\sigma_i$  in (3) and (4) by  $\sigma_{free}$ , since the actual conductivity of the nanosize metal inclusion might be lower than the bulk conductivity. Consequently,

$$\sigma_{skin} = \sigma_{free} \cdot f(\Delta); \text{ and } \delta(\omega) = \sqrt{\frac{2}{\omega\mu_i\mu_0\sigma_{free}}}. \quad (8)$$

### 2.3. Drude Model for Metals at Optical Frequencies

It is known that the frequency dependence of metals over the optical frequency range is described by the Drude model [12–15].

$$\varepsilon_i(j\omega) = 1 - \frac{\omega_p^2}{\omega(\omega - j\gamma)}, \quad (9)$$

where  $\omega_p$  is the angular plasma frequency for free electrons, and  $\gamma$  is the angular relaxation frequency. The relaxation frequency is  $\gamma = 1/\tau$ , where  $\tau$  is the resonance relaxation parameter. From (9), real and imaginary parts of complex permittivity are

$$\begin{aligned} \varepsilon_i(j\omega) &= \varepsilon'_i - j\varepsilon''_i; \\ \varepsilon'_i &= 1 - \frac{\omega_p^2}{\omega^2 + \gamma^2}; \\ \varepsilon''_i &= 1 - \frac{\omega_p^2\gamma}{\omega(\omega^2 + \gamma^2)} \end{aligned} \quad (10)$$

The imaginary part in (10) can be represented as usual

$$\varepsilon''_i = \frac{\sigma_D}{\omega\varepsilon_0}, \quad (11)$$

where Drude conductivity is

$$\sigma_D = \frac{\varepsilon_0\omega_p^2\gamma}{(\omega^2 + \gamma^2)}. \quad (12)$$

The total conductivity of a metal particle is comprised of “low-frequency” conductivity and Drude conductivity that is substantial at the higher optical frequencies. These two conductivities contribute to the total permittivity independently, because their effects are separated in frequency.

$$\begin{aligned} \varepsilon_i(j\omega) &= \varepsilon'_i - j\varepsilon''_i; \\ \varepsilon'_i &= \varepsilon'_D + \varepsilon'_{skin} = 1 - \frac{\omega_p^2}{\omega^2 + \gamma^2} + \frac{\sigma''_{skin}}{\omega\varepsilon_0}; \\ \varepsilon''_i &= \varepsilon''_D + \varepsilon''_{skin} = \frac{\omega_p^2\gamma}{\omega(\omega^2 + \gamma^2)} + \frac{\sigma'_{skin}}{\omega\varepsilon_0} = \frac{\sigma_\Sigma}{\omega\varepsilon_0}; \\ \sigma_\Sigma &= \sigma_D + \sigma'_{skin} \end{aligned} \quad (13)$$

Data for the plasma frequency and Drude relaxation frequency for metals can be taken from the graphs and tables in papers [14, 15]. In these papers, the Drude model parameters  $\omega_p$  and  $\gamma$  are given in  $[\text{cm}^{-1}]$  units, so that  $\omega[1/\text{cm}] = \frac{\omega[\text{rad/s}] \cdot 10^{-2}}{2\pi \cdot c[\text{m/s}]}$ .

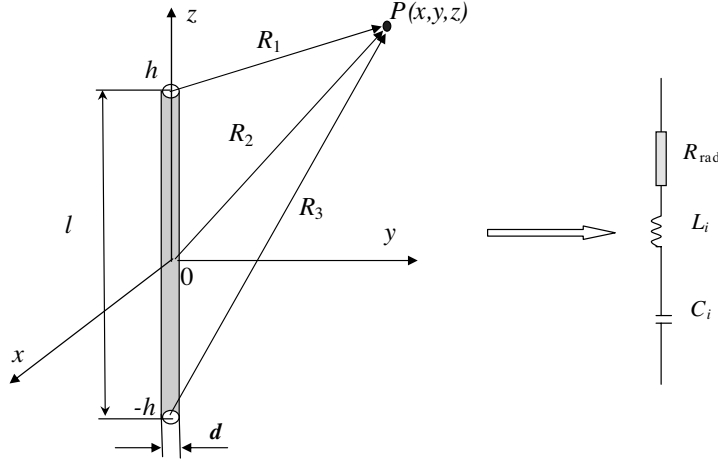


**Figure 3.** Analogy of an inclusion particle and a dipole antenna.

#### 2.4. Dimensional Resonance in Metal Particles

Electromagnetic resonance in the particles of inclusions is another source of frequency-dependent properties of composites. An inclusion particle in the form of a nanorod can be represented as an electric dipole antenna (see Figure 3). Suppose that nanorods are non-interacting, corresponding to a sparse concentration of inclusions in the base material. Let us calculate the equivalent conductivity of an inclusion particle. This conductivity then can be used in Maxwell Garnett formulation for the effective permittivity.

According to [16, 17], any inclusion particle can be described by its antenna dipole input impedance. This is a series connection of radiation resistance  $R_{rad}$ , capacitance of the wire  $C_i$  and its inductance  $L_i$ .

$$Z_{in} = R_{rad} + j\omega L_i + \frac{1}{j\omega C_i}. \quad (14)$$

For a dipole antenna these values are approximately calculated as in [18],

$$\begin{aligned} R_{rad} &= 20\pi^2 \sqrt{\varepsilon_{ef}} \left(\frac{1}{\lambda_0}\right)^2, \text{ [Ohms];} \\ C_i &= \frac{\pi\varepsilon_0\varepsilon_{ef}l}{2\ln(2a)}, \text{ [F];} \\ L_i &= \frac{\mu_0 l}{6\pi} \left(\ln(2a) - \frac{11}{6}\right), \text{ [H].} \end{aligned} \quad (15)$$

It is known that if the inclusions are small compared with wavelength, their input impedance is mainly capacitive. Radiation resistance determines effectiveness of the dipole radiation, and it will contribute to the real part of the permittivity of the composite.

The rigorous formulation for radiation resistance and reactance of a dipole antenna of any length can be found in [19, Section 21.2], and these parameters can be calculated using numerical integration. Thus, the input impedance can be calculated as

$$Z_{in} = \frac{j\eta}{4\pi \sin^2 kh} \int_{-h}^h F(z) dz, \quad (16)$$

where the integrand is

$$F(z) = \left[ \frac{e^{-jkR_1}}{R_1} + \frac{e^{-jkR_2}}{R_2} - 2 \cosh kh \frac{e^{-jkR_0}}{R_0} \right] \sin(k(h - |z|)). \quad (17)$$

The distances are calculated as

$$\begin{aligned} R_0 &= \sqrt{(d/2)^2 + z^2}; \\ R_1 &= \sqrt{(d/2)^2 + (z - h)^2}; \\ R_2 &= \sqrt{(d/2)^2 + (z + h)^2}. \end{aligned} \quad (18)$$

In (16)–(18),  $\eta = 120\pi \sqrt{\frac{\mu_{ef}}{\varepsilon_{ef}}}$  (for a dielectric composite  $\mu_{ef} = 1$ ),  $h = l/2$  is an antenna half-length, and  $k = \frac{2\pi}{\lambda_{ef}} = \frac{2\pi}{\lambda_0} \sqrt{\varepsilon_{ef}}$  is the wave number in the effective medium. It should be mentioned that values of  $\varepsilon_{ef}$  in (15)–(17) are taken from calculating effective permittivity using the Maxwell Garnett formula (1) before the dipole antenna effect is taken into account.

In [16], the polarizability of dipole particles is introduced as

$$\alpha_{ee} = \frac{l_{ef}^2}{j\omega Z_{in}} [\text{F} \cdot \text{m}^2], \quad (19)$$

where  $l_{ef}$  is the effective dipole antenna length. For small dipoles, it can be assumed that  $l_{ef} \approx l/2$ . For dipoles with  $l = \lambda/2$ ,  $l_{ef} = 0.637(2l) = 1.274l$  [20, Section 9.2] For longer dipole antennas, the effective length is  $l_{ef} = 2.558l^2/\lambda$ . (The effective length of a dipole antenna is calculated through an equivalent antenna with a homogeneous current distribution along the dipole, and the same area under the current distribution function along the dipole length as in the initial antenna).



The conductivity of particles due to the dimensional resonance can be calculated by equating the effective permittivity of a sparse conglomerate of the identical conductive particles (neglecting the base material) with polarizability  $\alpha_{ee}$  and a concentration of  $n$  particles per unit volume,

$$\varepsilon = \varepsilon_0 \left( 1 + \frac{n}{\varepsilon_0} \alpha_{ee} \right) = \varepsilon_0 \left( \varepsilon' - j \frac{\sigma_{res}}{\omega \varepsilon_0} \right), \quad (20)$$

For cylindrical particles,

$$n = f_i/v_i = \frac{4f_i}{\pi d^2 l}, \quad [1/\text{m}^3]. \quad (21)$$

Then, the conductivity associated with the dimensional resonance is

$$\sigma_{res} = j\omega n \alpha_{ee}, \quad [\text{S/m}]. \quad (22)$$

Substituting (19) and (20) in (22), one can get the conductivity associated with the dimensional resonance as

$$\sigma_{res} = \frac{nl_{ef}^2}{Z_{in}} = \frac{4f_i l_{ef}^2}{\pi d^2 l Z_{in}}. \quad (23)$$

This is a complex value,  $\sigma_{res} = \sigma'_{res} + j\sigma''_{res}$ , and it can be added to the formula (13), describing the total conductivity  $\sigma_\Sigma$ . Its real part contributes to the loss in the material, and the imaginary contributes to the real part of the composite permittivity, associated with the phase velocity of electromagnetic wave propagation. This means that when  $\alpha_{ee}$  is real (no loss),  $Z_{in}$  is imaginary (purely reactive), and then  $\sigma_{res}$  is real and contributes to loss in the material. When  $\alpha_{ee}$  is imaginary (only loss),  $Z_{in}$  is real (pure radiation resistance), and then  $\sigma_{res}$  is imaginary and contributes to the real part of permittivity of the composite.

## 2.5. Frequency Characteristic of the Base Material

The frequency characteristics of the base material also have an impact on the frequency characteristics of the mixture. Depending on the base material used for making the composite, and the frequency range of its application, this base material can be modeled as a lossless nondispersive medium, as a lossy Debye material, as a resonance Lorentzian medium, or as their superposition.

The Debye frequency characteristic for a dielectric base material is

$$\varepsilon_b = \varepsilon_{\infty b} + \frac{\varepsilon_{sb} - \varepsilon_{\infty b}}{1 + j\omega\tau_D}, \quad (24)$$

where  $\varepsilon_{sb}$  and  $\varepsilon_{\infty b}$  are static and high-frequency (“optic”) relative permittivities of the material, and  $\tau_D$  is the Debye relaxation time. In the case of a Lorentzian material, it is described as

$$\varepsilon_b = \varepsilon_{\infty b} + \frac{(\varepsilon_{sb} - \varepsilon_{\infty b})\omega_{0b}^2}{\omega_{0b}^2 - \omega^2 + 2j\omega\delta_b}, \quad (25)$$

where  $\omega_{0b}$  is the angular resonance frequency of the base material, and  $(2\delta_b)$  is the resonance line width at  $-3$  dB level.

If the base material resonance is pronounced and comparatively narrow in the frequency range of interest (narrowband Lorentzian material, for which  $\omega_0 = \omega_p > (2\delta)$  [22]), it might have a great impact on the frequency-selective properties of the composite. If the dielectric is wideband Lorentzian ( $\omega_0 = \omega_p < (2\delta)$ ), then its behavior is very close to the Debye frequency dependence [22].

### 3. RESULTS OF COMPUTATIONS

A program in Matlab has been developed to calculate reflection and transmission coefficients from a slab of a composite material containing metal particles (nanorods). Below there are the modeled results that take into account all the abovementioned effects.

Figure 4 shows the reflectance and transmittance for a layer of the modeled composite material  $1\ \mu\text{m}$  thick. The input data for computations are the following: the bulk conductivity of silver particles is  $\sigma_i = 6.3 \cdot 10^7$  S/m; the coefficient  $\Lambda$  taking the mean free path into account is assumed to be  $\Lambda = 0.8$ ; the mean free path of electrons in silver is taken as  $40$  nm; the aspect ratio of the inclusions is  $a = 50$ ; the length of the particles  $l = 1\ \mu\text{m}$ ; and the diameter of the particles is assumed to be  $d = 20$  nm. The volume fraction of the inclusions is  $f_i = 0.7/a$ , which is below the percolation threshold estimated as  $p_c = 4.5/a$  [6]. The parameters for polymethylmethacrylate (PMMA) base material taken for these computations are the Debye parameters:  $\varepsilon_s = 2.2$ ,  $\varepsilon_\infty = 1.9$ , and  $\tau_D = 10^{-14}$  s. It should be mentioned that PMMA is known to be almost transparent in the visual frequency band (98% transparency), while in the UV range it is almost non-transparent (wideband Lorentzian behavior with  $\omega_0 \approx 2 \cdot 10^{16}$  Hz). The dispersive curves for PMMA at optical and UV frequencies can be found in [21].

The frequency dependence of reflectance, transmittance, and absorbance (magnitude, resonance frequency, and width of the resonance line) greatly depends on the Drude parameters for silver  $-\omega_p$  and  $\gamma$ . Skin effect plays an important part for comparatively low-frequency absorption and frequency selectivity. Resonance of the inclusions falls into the frequency range of interest and contributes

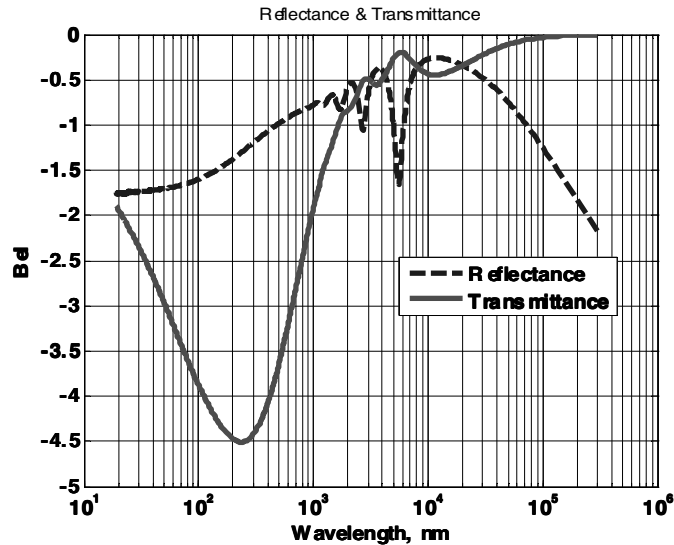


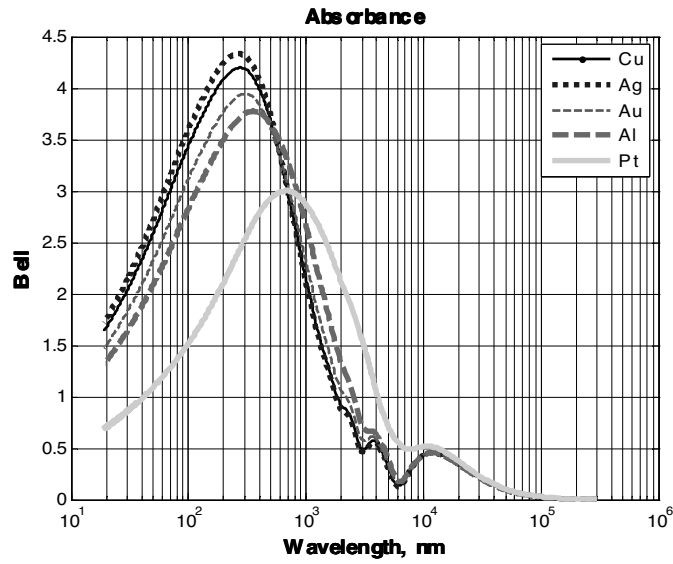
**Figure 4.** Reflectance and transmittance characteristics for a 1- $\mu\text{m}$ -thick slab of a composite material PMMA-Ag.

to the absorption and radiation by inclusion dipole antennas. This contribution is affected by the geometry of the inclusions.

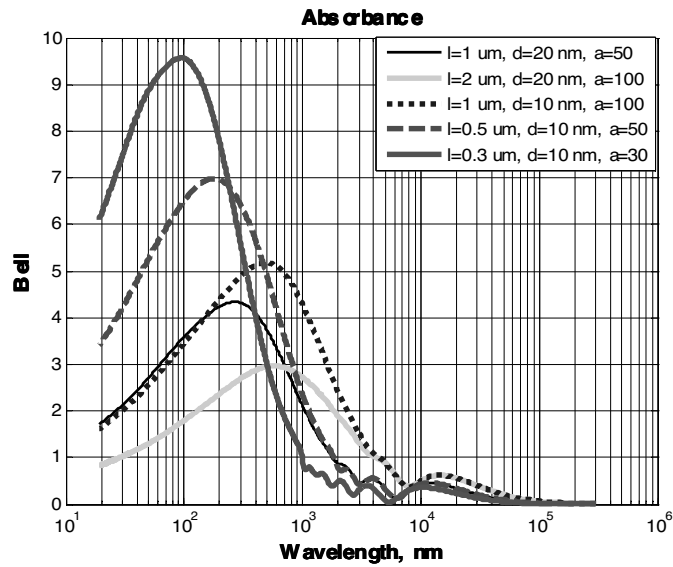
Figure 5 shows the influence of the material of inclusions on the absorbance, defined as  $A = \log_{10}(P_t/P_{inc})$  in bels. The Drude parameters for different metals—silver, copper, gold, aluminum, and platinum—are found in [15] and presented here in Table 1. The base material was PMMA, and the inclusion particles had an aspect ratio of  $a = 50$ , a length of  $l = 1 \mu\text{m}$ , and a diameter of  $d = 20 \text{ nm}$ . The volumetric fraction of the inclusions was  $f_i = 0.7/a$ . The composites containing metal particles with higher bulk conductivity will absorb energy more effectively.

Figure 6 shows that the absorbance characteristic can be also controlled by varying the size of the inclusions. It is important that the higher aspect ratio of inclusions does not necessarily yield greater absorbance, as happens with shielding effectiveness in the microwave range [2]. At optical frequencies, the longer particles of inclusions radiate more effectively than the shorter ones, and this radiation contributes to the real part of the effective permittivity of the composite, rather than its imaginary part responsible for absorption in the material.

Figure 7 demonstrates the effect of the length of inclusions on the absorbance. The diameter of inclusions for all the curves is



**Figure 5.** Absorbance for a  $1\ \mu\text{m}$ -thick slab of a composite material - PMMA base and different metals as inclusions.



**Figure 6.** Absorbance control by varying the size of inclusions. The volumetric fraction is  $f_i/7 = 0.7a$ . The layer thickness is  $1\ \mu\text{m}$ .

**Table 1.** Conductivity and Drude Model Parameters for Some Metals.

Metal	Bulk conductivity, $10^{-6} \cdot \sigma$ S/m	$10^{-12} \cdot \omega_p$ , 1/m	$10^{-12} \cdot \gamma$ , 1/m
Ag	63.05	1.369	27
Cu	57.0	1.122	13
Au	45.55	1.37	40
Al	36.5	2.24	120
Pt	9.59	0.78	105

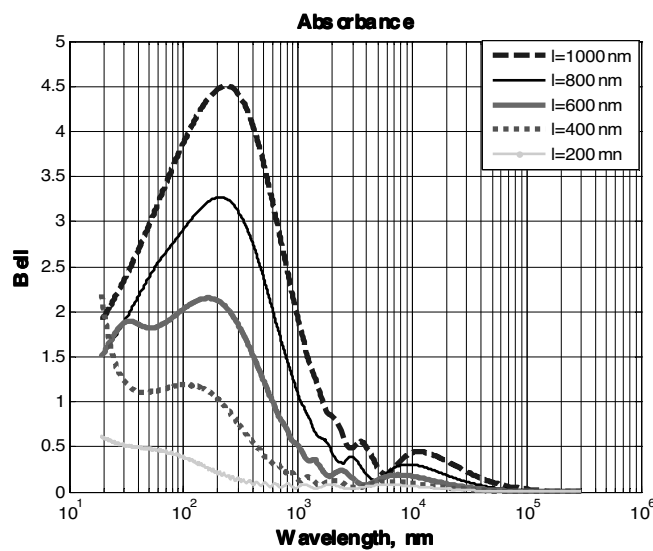


**Figure 7.** Absorbance as a function of wavelength for a  $1 \mu\text{m}$ -thick composite layer PMMA-Ag; parameter  $l$  is the length of Ag inclusions; the concentration of Ag particles constant at  $4.45 \cdot 10^{19} \text{ m}^{-3}$ .

20 nm. The dimensional resonance in the particles corresponds to the peak frequency of absorption. Thus, for particles having length  $l = 1000 \text{ nm}$ , the resonance frequency corresponds to a wavelength of about 375 nm. When particles are shorter, this peak shifts to the shorter wavelengths. The absorbance decreases in the frequency range of interest for shorter inclusions, since the number of Ag particles per unit volume (concentration) is kept constant ( $4.45 \cdot 10^{19} \text{ m}^{-3}$ ). Thus,

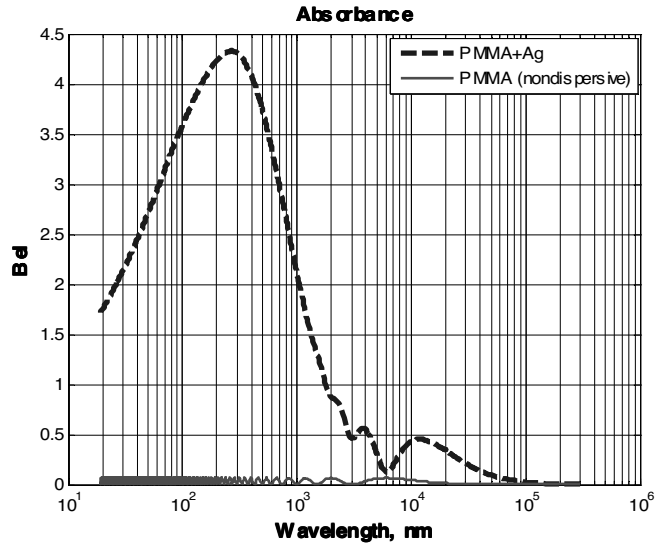


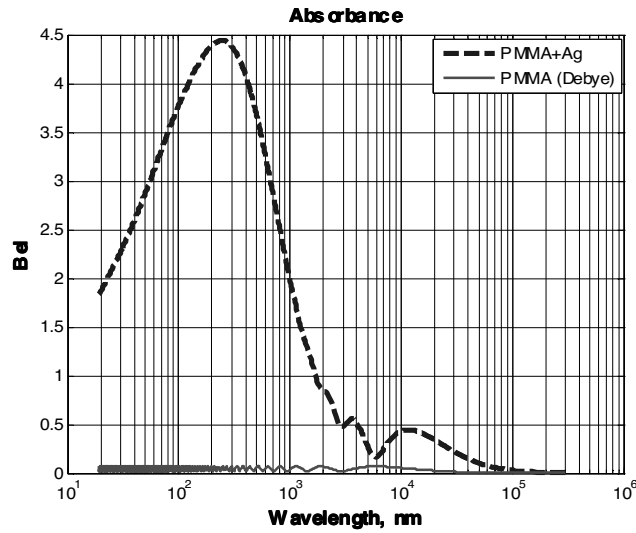
**Figure 8.** PMMA-nondispersive ( $\epsilon_{sb} = 2.2$ ); Ag particles ( $a = 50$ ;  $l = 1 \mu\text{m}$ ;  $d = 20 \text{ nm}$ ); concentration  $n_i = 4.45 \cdot 10^{19} \text{ m}^{-3}$ ; ( $f_i = 0.7/a$ ) for a  $1\text{-}\mu\text{m}$  thick slab.

the volumetric fraction of conducting inclusions decreases when they are shorter.

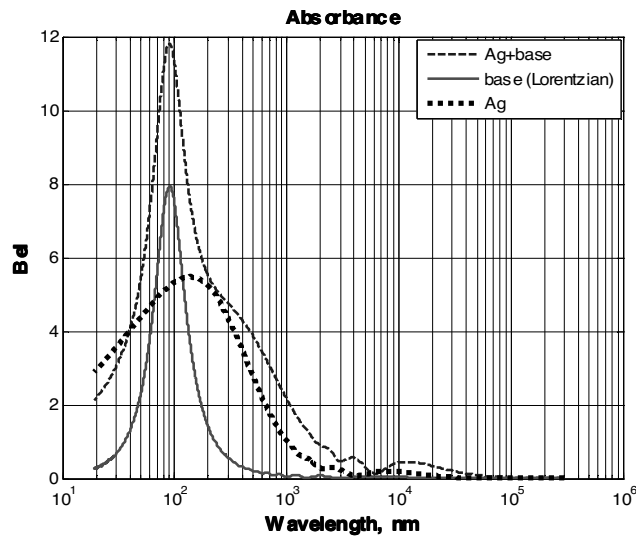
Figures 8 and 9 show the influence of Ag particles on the frequency characteristic of a mixture, when the model for PMMA base material is nondispersive (Figure 8) and is described by the Debye dispersion law (Figure 9). The base material itself is almost transparent in the frequency range of interest.

Figure 10 contains the absorbance characteristics for a Lorentzian-type base material, for a conglomerate comprised solely of Ag particles of the same size and volumetric fraction as in Figures 8 and 9, and the mixture of the base and the Ag inclusions. The frequency dependence for a composite is a superposition of the frequency characteristics of its phases. In reality, PMMA behaves more like a Lorentzian material in the UV range, where it becomes nontransparent. In the visual band, it is still appropriate to describe it as non-dispersive or slightly-dispersive with the Debye-like frequency dependence.

Figure 11 contains absorbance characteristics for composites with different Debye characteristics of the base material. In the graphs shown in the figure, the static permittivity is a varying parameter. It is seen that an increase of  $\epsilon_{sb}$  leads not only to the higher absorption in a wider band, but also to a shift of the peak absorption to shorter



**Figure 9.** PMMA-Debye ( $\epsilon_{sb} = 2.2$ ,  $\epsilon_{\infty b} = 1.9$ ,  $\tau_D = 1 \cdot 10^{-14}$  1/s); Ag particles ( $a = 50$ ;  $l = 1 \mu\text{m}$ ;  $d = 20$  nm); concentration  $n_i = 4.45 \cdot 10^{19} \text{ m}^{-3}$ ; ( $f_i = 0.7/a$ ) for a 1- $\mu\text{m}$  thick slab.



**Figure 10.** Dielectric-Lorentzian( $\epsilon_{sb} = 2.2$ ,  $\epsilon_{\infty b} = 1.9$ ,  $\omega_{0b} = \omega_{pb} = 2.05 \cdot 10^{16}$  rad/s;  $\delta_b = 1.67 \cdot 10^{16}$  rad/s); Ag particles ( $a = 50$ ;  $l = 1 \mu\text{m}$ ;  $d = 20$  nm); concentration  $n_i = 4.45 \cdot 10^{19} \text{ m}^{-3}$ ; ( $f_i = 0.7/a$ ) for a 1- $\mu\text{m}$  thick slab.

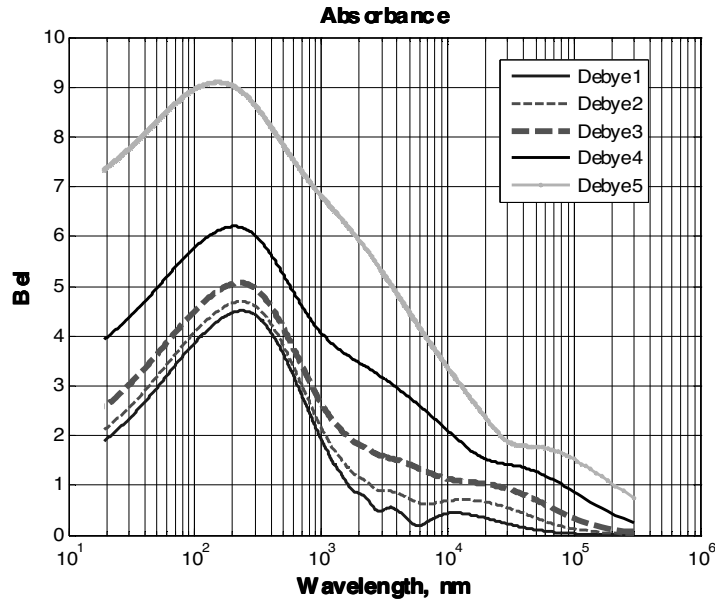


**Figure 11.** Ag particles ( $a = 50$ ;  $l = 1 \mu\text{m}$ ;  $d = 20 \text{ nm}$ ); concentration  $n_i = 4.45 \cdot 10^{19} \text{ m}^{-3}$  ( $f_i = 0.7/a$ ) for a  $1\text{-}\mu\text{m}$  thick slab for five different base materials, denoted as Debye1 through Debye5 corresponding to  $\varepsilon_{sb} = 2.2, 4.2, 8.2, 20.2,$  and  $50.2$ . The parameters  $\varepsilon_{\infty b} = 1.9$  and  $\tau_D = 1 \cdot 10^{-14} \text{ 1/s}$  are the same for all the five cases.

wavelengths. However, it can be seen that a substantial increase in  $\varepsilon_{sb}$  (from 2.2 to 8.2) does not significantly change the absorption characteristic.

Figure 12 shows the frequency dependence of absorbance, when different models of base materials are taken into account. There is almost no difference in the curves for PMMA model taken as the Debye (curve 1) and the wideband Lorentzian frequency dependence (curve 3). The size of the Ag particles was the same as in Figure 4 (aspect ratio  $a = 50$ , the length  $l = 1 \mu\text{m}$ , and the diameter  $d = 20 \text{ nm}$ ). The narrow absorption peak (curves 3 and 6) can be obtained using narrowband Lorentzian base material. This can be achieved at  $\omega_{0b} = \omega_{pb} > (2\delta)$ . If it is possible to find a dielectric with a Lorentzian peak at visible frequencies, then it would enhance the absorption by the silver particles. This problem might be solved, for example, by adding Ag particles in colored optical glass base [23].



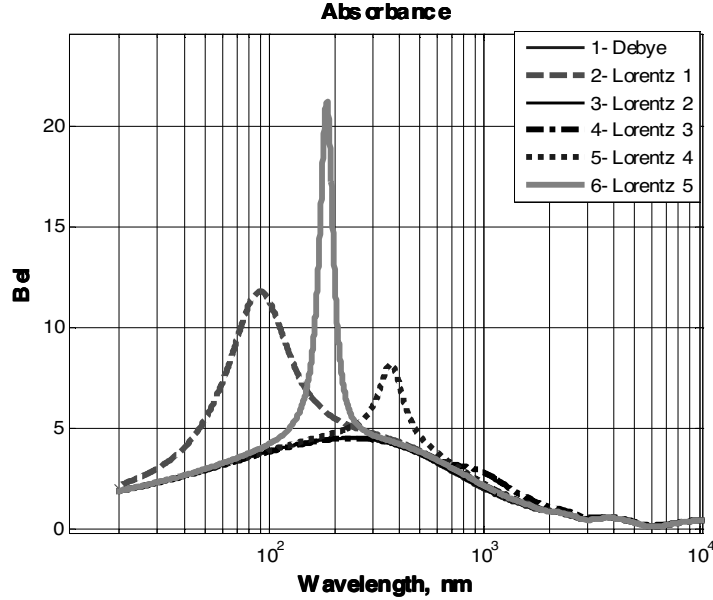


**Figure 12.** Ag particles ( $a = 50$ ;  $l = 1 \mu$ ;  $d = 20$  nm); concentration  $n_i = 4.45 \cdot 10^{19} \text{ m}^{-3}$  ( $f_i = 0.7/a$ ) for a  $1\text{-}\mu\text{m}$  thick slab with five different base materials: **1**-PMMMA-Debye; **2**-Lorentzian 1:  $\varepsilon_{sb} = 2.2$ ,  $\varepsilon_{\infty b} = 1.9$ ,  $\omega_{0b} = \omega_{pb} = 2.05 \cdot 10^{16}$  rad/s;  $\delta = 1.67 \cdot 10^{16}$  rads; **3**-Lorentzian 2:  $\varepsilon_{sb} = 2.2$ ,  $\varepsilon_{\infty b} = 1.9$ ,  $\omega_{0b} = \omega_{pb} = 2.05 \cdot 10^{15}$  rad/s;  $\delta = 1.67 \cdot 10^{16}$  rads; **4**-Lorentzian 3:  $\varepsilon_{sb} = 2.2$ ,  $\varepsilon_{\infty b} = 1.9$ ,  $\omega_{0b} = \omega_{pb} = 5.0 \cdot 10^{15}$  rad/s;  $\delta = 1.67 \cdot 10^{15}$  rads; **5**-Lorentzian 4:  $\varepsilon_{sb} = 2.2$ ,  $\varepsilon_{\infty b} = 1.9$ ,  $\omega_{0b} = \omega_{pb} = 2.05 \cdot 10^{15}$  rad/s;  $\delta = 1.67 \cdot 10^{15}$  rads; **6**-Lorentzian 5:  $\varepsilon_{sb} = 2.2$ ,  $\varepsilon_{\infty b} = 1.9$ ,  $\omega_{0b} = \omega_{pb} = 2.05 \cdot 10^{15}$  rad/s;  $\delta = 1.67 \cdot 10^{15}$  rads.

#### 4. CONCLUSION

Frequency-dependent parameters of composites containing 3D randomly oriented conducting inclusions (nanorods) at optical frequencies can be modeled using Maxwell Garnett formulation, if the concentration of inclusions is smaller than the percolation threshold. The frequency-dependent permittivity of a mixture mainly depends on the conductivity of the metal inclusions. Behavior of metal inclusions at optical frequencies greatly differs from that at microwave frequencies. Nanosize metal inclusions exhibit frequency dependence because of the skin-effect and free electron plasma resonance phenomena described by the Drude model. Also, an inclusion particle behaves as a resonant

scatterer, so its dipole antenna model should be taken into account. In addition, the mean free path of electrons in metals may be smaller than the characteristic size of metal inclusions, and this will substantially decrease the conductivity of the metals. All these effects are incorporated in the Maxwell Garnett mixing formulation, and give degrees of freedom for forming frequency characteristics of composite media containing conducting particles.

## ACKNOWLEDGMENT

This work was supported by the Air Force Research Laboratory under Contract FA8650-04-C-5704 through the Center for Advanced Materials Technology, University of Missouri-Rolla.

## REFERENCES

1. Maxwell, G., J. C., "Colours in metal glasses and metal films," *Philos. Trans. R. Soc. London, Sect. A*, Vol. 3, 385–420, 1904.
2. Koledintseva, M. Y., P. C. Ravva, R. E. DuBroff, J. L. Drewniak, K. N. Rozanov, and B. Archambeault, "Engineering of composite media for shields at microwave frequencies," *Proc. IEEE EMC Symposium*, Vol. 1, 169–174, Chicago, IL, August 2005.
3. Koledintseva, M. Y., J. Wu, J. Zhang, J. L. Drewniak, and K. N. Rozanov, "Representation of permittivity for multi-phase dielectric mixtures in FDTD modeling," *Proc. IEEE Symp. Electromag. Compat.*, Vol. 1, 309–314, Santa Clara, CA, August 9–13, 2004.
4. Matitsine, S. M., K. M. Hock, L. Liu, et. al., "Shift of resonance frequency of long conducting fibers embedded in a composite," *J. Appl. Phys.*, Vol. 94, No. 2, 1146–1154, 2003.
5. Huang, J., M. Y. Koledintseva, P. C. Ravva, J. L. Drewniak, R. E. DuBroff, B. Archambeault, and K. N. Rozanov, "Design of a metafilm-composite dielectric shielding structure using a genetic algorithm," *Proc. Progress in Electromagnetic Research Symposium (PIERS)*, 241–245, Cambridge, MA, USA, March 26–29, 2006.
6. Lagarkov, A. N. and A. K. Sarychev, "Electromagnetic properties of composites containing elongated conducting inclusions," *Phys. Review B*, Vol. 53, No. 9, 6318–6336, March 1996.
7. Landau, L. D., E. M. Lifshitz, and L. P. Pitaevskii, *Electrodynamics of Continuous Media*, 2nd ed., Oxford, Pergamon, New York, 1984.

8. Gottlieb, D. and V. Halpern, "The electrical conductivity of very thin metal films," *J. Phys. F: Metal. Phys.*, Vol. 6, No. 12, 2333–2339, 1976.
9. Chen and D. Gardner, "Influence of line dimensions on the resistance of Cu interconnections," *IEEE Electr. Dev. Lett.*, Vol. 19, No. 12, 508, 1998.
10. Kapur, P., J. P. McVittie, and K. C. Saraswat, "Technology and reliability constrained future copper interconnects — Part I: Resistance modeling," *IEEE Trans. Electr. Dev.*, Vol. 49, No. 4, 590–597, 2002.
11. Im, S., N. Srivastava, K. Banerjee, and K. Goodson, "Thermal scaling analysis of multilevel C/low-k interconnect structures in deep nanometer scale technologies," *Proc. 22th Int. VLSI Multilevel Interconnect Conf. (VMIC)*, 525–530, Fremont, CA, Oct. 3–6, 2005.
12. Zhang, R., S. Dods, and P. Catrysse, "FDTD approach for optical metallic material," *Laser Focus World*, 68, July 2004 ([www.laserfocusworld.com](http://www.laserfocusworld.com)).
13. Veronis, G., R. W. Dutton, and S. Fan, "Metallic photonic crystals with strong broadband absorption at optical frequencies over wide angular range," *J. Appl. Phys.*, Vol. 97, No. 9, 2005.
14. Ordal, M. A., L. L. Long, R. J. Bell, S. E. Bell, R. R. Bell, R. W. Alexander, Jr., and C. A. Ward, "Optical properties of the metals Al, Co, Au, Fe, Pb, Ni, Pd, Pt, Ag, Ti, and W in the infrared and far infrared," *Appl. Optics*, Vol. 22, No. 7, 4493–4499, April 1983.
15. Ordal, M. A., R. J. Bell, R. W. Alexander, Jr., L. L. Long, and M. R. Querry, "Optical properties of the metals Al, Co, Au, Fe, Pb, Ni, Pd, Pt, Ag, Ti, and W in the infrared and far infrared," *Appl. Optics*, Vol. 24, No. 24, 1099–1120, Dec. 1985.
16. Tretyakov, S. A., F. Mariotte, C. R. Simovski, T. G. Kharina, and J.-P. Heliot, "Analytical antenna model for chiral scatterers: comparison with numerical and experimental data," *IEEE Trans. Antennas and Propagat.*, Vol. 44, No. 7, 1006–1014, July 1996.
17. Tretyakov, S. A., "Metamaterials with wideband negative permittivity and permeability," *Microw. Opt. Techn. Lett.*, Vol. 31, No. 3, 163–165, Nov. 2001.
18. King, R. W. P. and C. W. Harrison, *Antennas and Waves: A Modern Approach*, MIT Press, Cambridge, MA, 1969.
19. Orfanidis, S. J., *Electromagnetic Waves and Antennas*, published on website [www.ece.rutgers.edu/orfanidi/ewa](http://www.ece.rutgers.edu/orfanidi/ewa)

20. Sazonov, D.M., *Antennas and Microwave Devices*, Vysshaya Shkola, Moscow, Russia, 1988.
21. Risko, J. J., L. J. Brillson, R. W. Bigelow, and T. J. Fabish, "Electron energy loss spectroscopy and the optical properties of polymethylmethacrylate from 1 to 300 eV," *J. Chem Phys.*, Vol. 69, No. 9, 3931–3939, Nov. 1978.
22. Koledintseva, M. Y., J. L. Drewniak, D. J. Pommerenke, K. N. Rozanov, G. Antonini, and A. Orlandi, "Wideband lorentzian media in the FDTD algorithm," *IEEE Trans. Electromag. Compat.*, Vol. 47, No. 2, 392–398, May 2005.
23. Colored Optical Glass, [http://www.lzos.ru/en/glass\\_color.htm](http://www.lzos.ru/en/glass_color.htm)